

# Source model composed of asperities for the 2004 Mid Niigata Prefecture, Japan, earthquake ( $M_{\text{JMA}}=6.8$ ) by the forward modeling using the empirical Green's function method

K. Kamae<sup>1</sup>, T. Ikeda<sup>2</sup>, and S. Miwa<sup>2</sup>

<sup>1</sup>Research Reactor Institute, Kyoto University, Osaka 590-0494, Japan

<sup>2</sup>Technical Research Institute, Tobishima Corp., Chiba 270-0222, Japan

(Received February 12, 2005; Revised April 28, 2005; Accepted May 2, 2005)

A preliminary source model composed of asperities for the 2004 Mid Niigata Prefecture, Japan, earthquake ( $M_{\text{JMA}}=6.8$ ) was estimated by the empirical Green's function method. The source parameters for two asperities located on the fault plane were determined from the comparisons of the synthesized broad-band ground motions with the observed ones at several stations including near source. Furthermore, we performed the preliminary nonlinear analysis of the sedimentary soils to reproduce the observed ground motions at NIG019 of K-NET. Resultantly, we pointed out the need of more asperity in northern part on the fault plane and the importance of the quantitative analysis of the nonlinearity of the sedimentary soils at K-NET stations.

**Key words:** Source model, asperity, forward modeling, empirical Green's function method, nonlinear analysis.

## 1. Introduction

On 23th October 2004, the Mid Niigata Prefecture, Japan, earthquake ( $M_{\text{JMA}}=6.8$ ) struck the Chuetsu district in Niigata Prefecture, and caused the heavy damages since the 1995 Hyogo-ken Nanbu earthquake. In this earthquake, destructive strong ground motions showing the instrumental seismic intensity 7 by the Japan Meteorological Agency (JMA), which is the maximum seismic intensity in Japan, have been recorded at strong-motion observation stations in the near-source area. The understanding of the source characteristics for explaining such broad-band strong ground motion recordings is very important for the strong ground motion prediction to mitigate seismic disasters from future large earthquakes. This paper provides a preliminary source model for the 2004 Mid Niigata Prefecture earthquake estimated by the empirical Green's function method (Irikura, 1986). The advantage of this method is that it includes the propagation path and local site effects and estimates basically broad-band ground motions as long as the aftershock recordings are accurate enough in broad-frequency band. Furthermore, this method is convenient and robust in case of having many aftershock recordings as the empirical Green's functions and having difficulty in calculating the theoretical Green's functions because of complicated underground structure around the corresponding region. In our simulation, we determine a source model composed of asperities which is capable of reproducing broad-band strong ground motions using a forward modeling approach. We assume that ground motions are generated from two asperities, each of which has a uniform stress drop with a finite extent on the

fault plane and obeys an  $\omega^{-2}$  spectral scaling. Their locations are basically determined referring to the inverted slip models, e.g., by Honda *et al.* (2005). This procedure is the same as Kamae and Irikura (1998) and Kamae and Kawabe (2004).

## 2. Strong Ground Motion Data

We used broad-band acceleration data at five stations (NIG017, NIG019, NIG020, NIG021, NIG022) by K-NET of the National Research Institute for Earth Science and Disaster Prevention. The locations of these stations are shown in Fig. 1 together with the epicenters and the focal mechanisms of the mainshock and the aftershocks used here as the empirical Green's functions. Table 1 and Table 2 show the information of the mainshock and the aftershocks, respectively. We used Aftershock-1 for synthesizing the ground motion from Asp-1 at NIG017, NIG019, NIG021, NIG022, and for Asp-2 at NIG017, Aftershock-2 for Asp-2 at NIG019, NIG021, NIG022, Aftershock-3 for Asp-1 and Asp-2 at NIG020. We selected the aftershocks as the empirical Green's functions from these locations and the existence of recordings. The source parameters (fault area and stress drop) of the aftershocks were estimated roughly from the displacement source spectra calculated by the borehole data of KiK-net which are not affected strongly by the reflected wave from the surface. We used the aftershock data bandpass-filtered (0.3–10.0 Hz at NIG017, 0.5–10.0 Hz at NIG019 and NIG020, 0.2–10.0 Hz at NIG021 and NIG022) depending on the quality of each aftershock waveform data.

## 3. Source Model and Synthetics

Several inverted source models have already been estimated from teleseismic data or/and strong ground motion data (e.g. Honda *et al.*, 2005; Hikima and Koketsu,

Copy right© The Society of Geomagnetism and Earth, Planetary and Space Sciences (SGEPSS); The Seismological Society of Japan; The Volcanological Society of Japan; The Geodetic Society of Japan; The Japanese Society for Planetary Sciences; TERRAPUB.

Table 1. Information of the mainshock.

Mainshock	
Origin time (JST)	2004/10/23 17:56
Latitude (deg)	37.292
Longitude (deg)	138.867
Depth (km)	13.1
$M_{JMA}$	6.8
Seismic moment (Nm)*	$7.53 \times 10^{18}$
Focal mechanism solution*	212/93/47
Strike/rake/dip	27/87/43

\* F-net

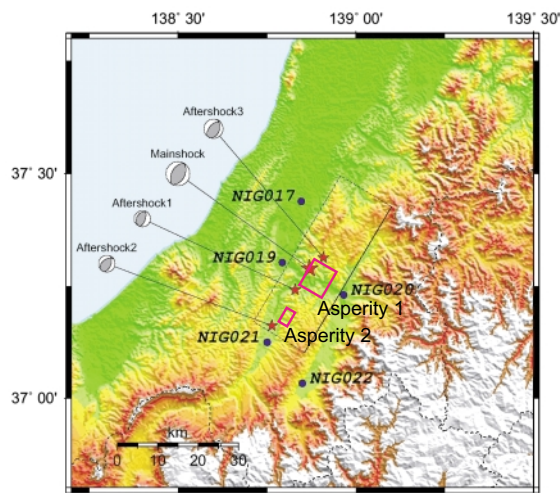


Fig. 1. Map showing the K-NET and JMA observation station locations and epicenters of the mainshock and the aftershocks used as the empirical Green's functions and source model consisting of two asperities estimated from forward modeling using the empirical Green's function method. Fault plane of the mainshock has strike of  $211^\circ$  and dip angle of  $52^\circ$ .

2005). Figure 2 is the inverted source model by Honda *et al.* (2005). As you can see in this figure, the region with relatively large slip exists near the hypocenter. This feature is similar to another model. In this study, we initially referred to these results to determine the locations of the asperities which generate strong ground motions. Result-

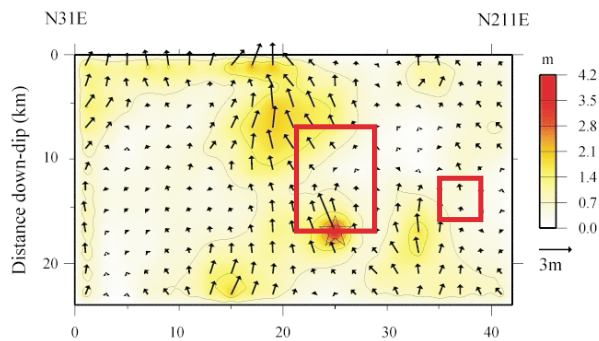


Fig. 2. Source model composed of two asperities. The model is superimposed the inverted slip contours by Honda *et al.* (2005).

tantly, as shown in Fig. 2, the first asperity (Asp-1) is located near the rupture nucleation point (hypocenter); the second (Asp-2) in the deeper part of south-west direction of the hypocenter, although Asp-2 can not be found in the inverted slip models derived from data that have been low-pass-filtered (about 1 Hz). As mentioned below, the reason why Asp-2 is needed is to reproduce high-frequency ground motions with large peak acceleration recorded at south observation stations (NIG021 and NIG022). Our objective is to determine a source model capable of explaining broadband motions containing low- and high-frequency components. To accomplish this, we assumed a simplified source model composed of asperities located on two regions shown in Fig. 2. We assumed that the ground motions should be generated only from the two subevents that correspond to Asp-1 and Asp-2. We adjusted the locations, sizes, and stress parameters of those two subevents to fit the simulated motions to the observed ones using a forward modeling approach. The dimensions of these asperities specifying basically the waveform (envelope) have been determined by the number of divisions and the areas of the aftershocks used as the empirical Green's functions. Here, the number of divisions and the stress parameters specifies the levels of the synthetic high- and low- frequency ground motions. We searched the parameters to obtain a better fit of the envelope and high frequency level between synthetics and observed broadband ground motions. We assumed an  $S$ -wave velocity of 3.5 km/s along the wave propagation path and a rup-

Table 2. Aftershocks and source parameters.

	Aftershock-1	Aftershock-2	Aftershock-3
Origin time (JST)	2004/10/24 14:21	2004/10/25 01:27	2004/10/23 23:34
Latitude (deg)	37.242	37.162	37.314
Longitude (deg)	138.829	138.764	138.909
Depth (km)	11.5	6.3	19.9
$M_{JMA}$	4.7	4.5	5.4
Seismic moment (Nm)*	$1.36 \times 10^{16}$	$4.16 \times 10^{15}$	$4.14 \times 10^{16}$
Fault area (km <sup>2</sup> )	6.0	4.5	4.5
Stress drop (MPa)	2.3	1.0	10.5
Focal mechanism solution*	20/84/62	21/66/51	223/106/55
Strike/Rake/Dip	213/101/28	236/116/45	17/69/38

\* F-net

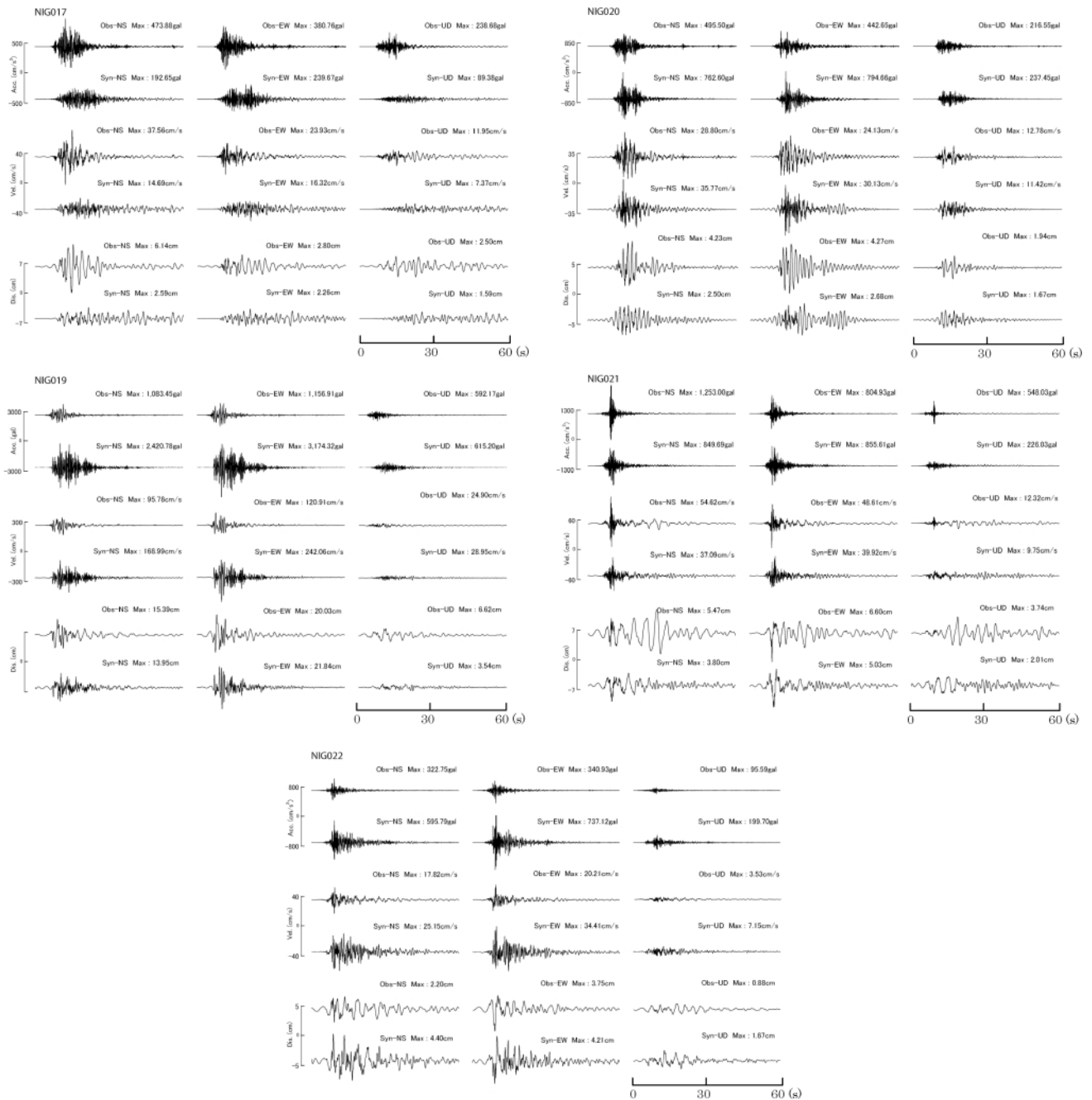


Fig. 3. Comparison between the synthesized and observed motions at NIG017, NIG019, NIG020, NIG021, and NIG022.

ture velocity of 2.0 km/s on the fault plane referring to the source inversions. Furthermore, we assumed that the rupture should start from the center bottom inside Asp-1 and propagate radially. The rupture of Asp-2 should restart from the northeast bottom after the rupture reaches that point and propagate radially.

After several trials, we obtained the best source model shown in Fig. 1 and Fig. 2. The source parameters for each asperity are summarized in Table 3. Here, the size and stress parameter for Asp-1 were determined to match the recordings at NIG019 and NIG020 in near-source region. On the other hand, the source parameters for Asp-2 was determined to match the high-frequency recordings with large peak acceleration at NIG021 and NIG022. The stress parameters (stress drop) of asperities are close to those for

the 1995 Hyogo-ken Nanbu earthquake (about 10 MPa to 20 MPa) by Kamae and Irikura (1998) as well as the averaged ones (about 12 MPa) for past inland earthquakes. The synthesized motions at five stations are compared with the observed ones in Fig. 3. Figure 4 shows the comparison between the synthetic and observed pseudo-velocity response spectra (PVRs) with a damping factor of 0.05.

#### 4. Discussion

From Fig. 3 and Fig. 4, you firstly can see that the synthetics at NIG021 and NIG022 are in agreement with the observed ones. Separate contributions of Asp-1 and Asp-2 at NIG021 shown in Fig. 5 show a need to reproduce the large acceleration recording. Next, at NIG017 located in north direction, the synthetics are slightly underestimated

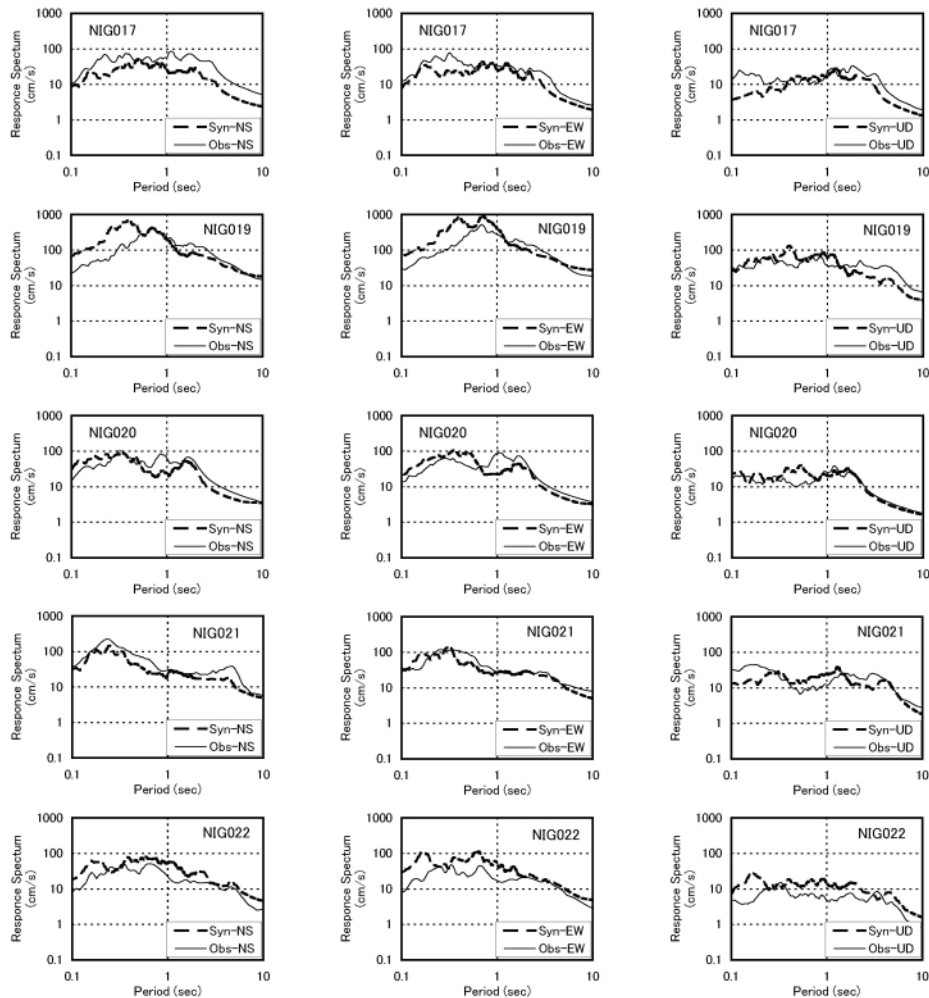


Fig. 4. Comparison of the pseudo-velocity response spectra (PVRs) with damping factor of 0.05 of the synthesized motions and those of the observed motions at six sites. Bold dotted line shows the PVRs of the synthesized motions. Solid thin line shows the PVRs of the observed motions.

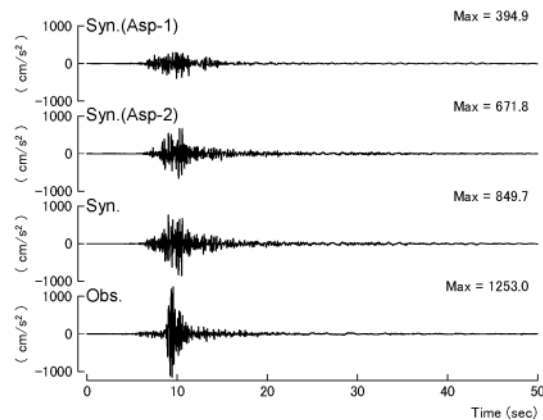


Fig. 5. Separate contributions of Asp-1 and Asp-2 to the synthetics at NIG021.

compared with the observed ones. This result might suggest the existence of more asperity located in northern part on the fault plane. We need to investigate not only the possibility of more asperity but also the validation of the aftershocks as the empirical Green's functions. Because we did not consider the difference of the radiation pattern between

Table 3. Source parameters for each asperity.

	$M_0$ (Nm)	L (km)×W (km)	$\Delta\sigma$ (MPa)
Asp-1	$2.60 \times 10^{18}$	$7.5 \times 10.0$	7.0
Asp-2	$5.28 \times 10^{17}$	$4.0 \times 4.0$	20.0

the Asp-1 and the aftershock in this study. Finally, we can point out that the synthetic acceleration and velocity ground motions in horizontal components at NIG019 are extremely overestimated compared with the observed ones in spite of good matching at NIG020 located near source.

The effect of nonlinearity of the sedimentary soils at NIG019 is pointed out from the existence of the extended predominant period appeared in acceleration recording. Here, in order to investigate the reason of the overestimation in synthetics, we perform the preliminary nonlinear simulation at NIG019 based on the velocity structure by K-NET soil information and the spectral inversion results by Kawase and Matsuo (2004). The nonlinearity is modeled as follows. The skeleton curve of stress-strain is represented by the Ramberg-Osgood model (Jennings, 1964), and the Masing rule is applied to the hysteretic characteristics re-

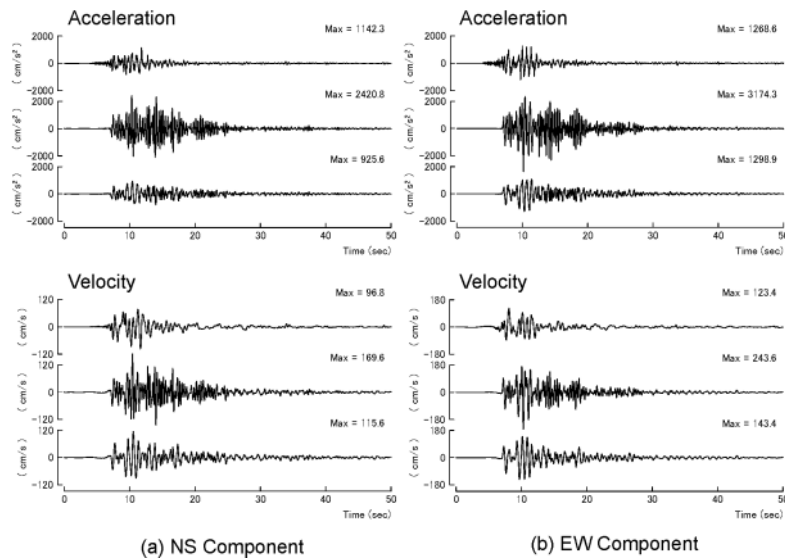


Fig. 6. Comparison of the synthetics considering the nonlinearity of sedimentary soils and the observed ones at NIG019. Top: observation. Middle: synthetic by linear analysis. Bottom: synthetic by nonlinear analysis.

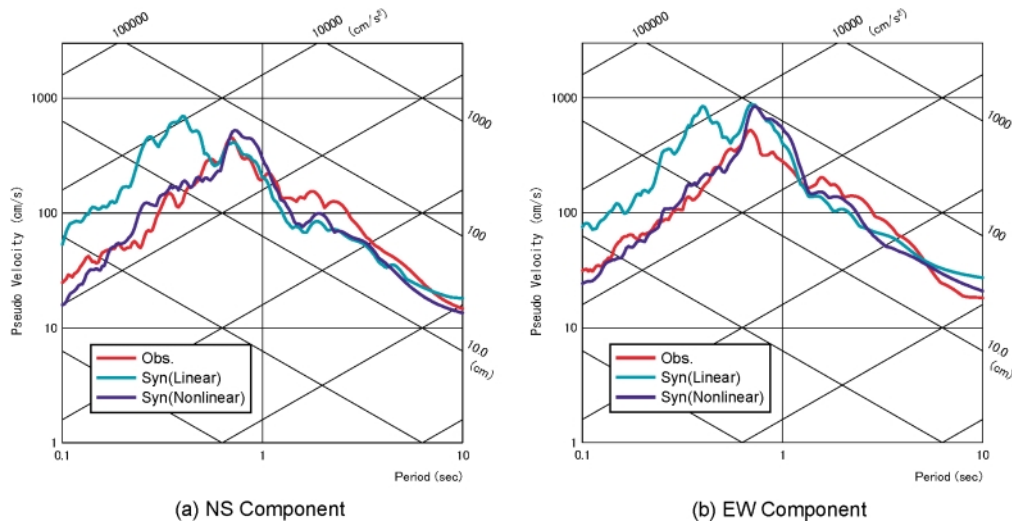


Fig. 7. Comparison of the PVRs's for the synthetic and the observed motions shown in Fig. 6.

Table 4. Model parameters for nonlinear soil response analysis at NIG019.

Layer	Thickness (m)	Density (t/m <sup>3</sup> )	$V_s$ (m/s)	$Q$	R-O Model		$N$
					$\gamma_{0.5}$	$h_{\max}$	
1	3	1.65	150	25	0.0005	0.20	3
2	6	1.90	380	50	0.0003	0.24	3
3	4	1.95	580	50	0.0004	0.24	2
4	15	1.90	340	50	0.0006	0.24	5
5	80	2.10	1300	100	0.0015	0.28	8
Base	—	2.20	3000	500	—	—	—

$\gamma_{0.5}$  is the shear strain  $G/G_0$  is equal to 0.5. Where,  $G$  is shear modulus and  $G_0$  is elastic shear modulus.  $h_{\max}$  is damping factor in infinite shear strain.  $N$  is the number of division in each layer to increase the accuracy of non-linear calculation.

lation. The parameters needed in simulation are summarized in Table 4. First of all, the input motions on base-rock are calculated from the synthesized acceleration motions at the surface shown in Fig. 3 using the Haskell's matrix

method (Haskell, 1953). Next, we synthesize the acceleration and velocity motions including the nonlinearity at the surface imposing the estimated input motions on base-rock. In Fig. 6, the results of the simulation are compared with



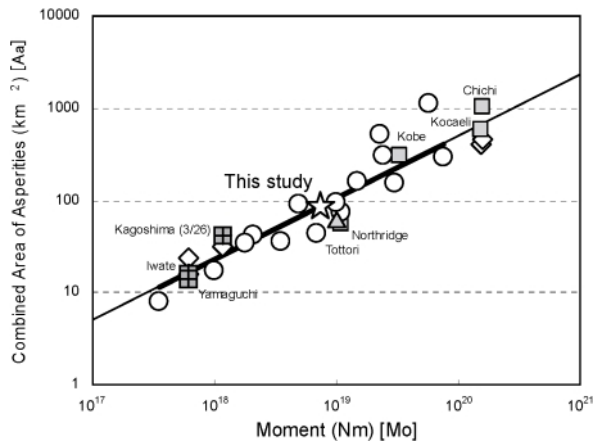


Fig. 8. Relation between the seismic moment and the combined area of asperities for this event. Star mark (☆) is superimposed the relations for the past inland earthquakes (Somerville *et al.*, 1999; Miyakoshi *et al.*, 2000).

the observed acceleration and velocity motions. Generally speaking, the simulated ground motions fit acceptably the observed ones in both components. The maximum strain is about 2% in the fourth layer. In Fig. 7, you can see that the discrepancy between the synthetic pseudo velocity response spectra and the observed ones are improved by considering the nonlinearity of the sedimentary soils. Moreover, there is a possibility for appearance of cyclic mobility in the records of NIG019 because spikes can be seen in the waveforms. It should be considered the nonlinearity of sedimentary soil depends not only on shear strain of soil but also reduction of confining pressure from the increasing of excess pore water pressure.

These results also show the validation of the source model estimated here. We need to do the same simulations to investigate the reason of the overestimation at NIG020 as well as NIG022.

Finally, we show the relation between the seismic moment and the combined asperity area for this event in Fig. 8 superimposing Somerville *et al.* (1999) and Miyakoshi *et al.* (2000). You can see that this event is consistent with the average of the past inland earthquakes.

## 5. Conclusions

We tried to estimate the source model composed of two asperities by the forward modeling using the empirical

Green's function method. Finally, we determined the source parameters for the asperities located on the fault plane from the comparisons between the broad-band strong ground motions synthesized considering the nonlinearity of the sedimentary soils and the observed ones. We need to revise the estimates of the source parameters for asperities after the detailed analysis including the more accurate nonlinear calculation of the sedimentary soils.

**Acknowledgments.** We thank the National Research Institute for Earth Science and Disaster Prevention for providing us with K-NET and KiK-net strong ground motion data. This study was partially supported by Special Coordination Funds, titled "Study on the master model for strong ground motion prediction toward earthquake disaster mitigation" of the Ministry of Education, Science, Sports, and Culture, Japan. We greatly appreciate the useful suggestions and comments by two reviewers.

## References

- Haskell, N. A., The dispersion of surface waves on multilayered media, *Bull. Seism. Soc. Am.*, **43**, 17–34, 1953.
- Hikima, K. and K. Koketsu, The rupture processes, in it 2004 Chuetsu, Niigata, earthquake: Strong motions and rupture processes, <http://taro.eri.u-tokyo.ac.jp/saigai/chuetsu/chuetsu.html>, 2005.
- Honda, R., S. Aoi, N. Morikawa, H. Sekiguchi, T. Kunugi, and H. Fujiwara, Ground motion and rupture process of the 2004 Mid Niigata Prefecture earthquake obtained from strong motion data of K-NET and KiK-net, *Earth Planets Space*, **57**, this issue, 527–532, 2005.
- Irikura, K., Prediction of strong ground acceleration motions using empirical Green's function, Proc. 7th Japan Earthq. Eng. Symp., 151–156, 1986.
- Jennings, P. C., Periodic response of a general yielding structures, Proc. ASCE, EM Div., Vol. 90, Apr., 1964.
- Kamae, K. and K. Irikura, Source model of the 1995 Hyogo-ken Nanbu earthquake and simulation of near-source ground motion, *Bull. Seism. Soc. Am.*, **88**(2), 400–412, 1998.
- Kamae, K. and H. Kawabe, Source model composed of asperities for the 2003 Tokachi-oki, Japan, earthquake ( $M_{JMA}=8.0$ ) estimated by the empirical Green's function method, *Earth Planets Space*, **56**(3), 323–327, 2004.
- Kawase, H. and H. Matsuo, Relationship of S-wave velocity structure and site effects separated from the observed strong motion data of K-NET, KiK-net, and JMA network, *J. of JAEE*, **4**(4), 126–145, 2004.
- Miyakoshi, K., T. Kagawa, H. Sekiguchi, T. Iwata, and K. Irikura, Source characterization of inland earthquakes in Japan using source inversion results, Proc. 12th WCEE, New-Zealand, (CD-ROM), 2000.
- Somerville, P. G., K. Irikura, R. Graves, S. Sawada, D. Wald, N. Abrahamson, Y. Iwasaki, T. Kagawa, N. Smith, and A. Kowada, Characterizing crustal earthquake slip models for the prediction of strong ground motion, *Seismological Research Letters*, **70**, 59–80, 1999.

K. Kamae (e-mail: kamae@kuca.rii.kyoto-u.ac.jp), T. Ikeda, and S. Miwa